Constructing "petal" modes from the coherent superposition of Laguerre-Gaussian modes

Darryl Naidoo[a,b], Andrew Forbes[a,b†], Kamel Aït-Ameur[c] and Marc Brunel[d]
[a]CSIR National Laser Centre, P. O. Box 395, Pretoria 0001, South Africa
[b]School of Physics, University of KwaZulu-Natal, Private Bag X54001, Durban 4000, South Africa
[c]CIMAP—ENSICAEN, 6, bd Maréchal Juin, 14050 Caen Cedex 4, France
[d]CORIA UMR 6614, Université de Rouen, Avenue de l'université BP 12, 76801 Saint Etienne du Rouvray Cedex, France

ABSTRACT

An experimental approach in generating Petal-like transverse modes, which are similar to what is seen in porro-prism resonators, has been successfully demonstrated. We hypothesize that the petal-like structures are generated from a coherent superposition of Laguerre-Gaussian modes of zero radial order and opposite azimuthal order. To verify this hypothesis, visually based comparisons such as petal peak to peak diameter and the angle between adjacent petals are drawn between experimental data and simulated data. The beam quality factor of the Petal-like transverse modes and an inner product interaction is also experimentally compared to numerical results.

Keywords: Petal-like transverse modes, Laguerre-Gaussian, Coherent superposition.

1. INTRODUCTION

Solid-state porro prism laser resonators are an adaptation of conventional flat-flat laser cavities where the flat mirrors are replaced with right angle prisms. These prisms, which are often referred to as porro prisms, have a valuable property that, independent of angle of incidence, all rays incident on the prism are reflected back parallel to the initial propagation direction. This property allows for this laser configuration to be insensitive to misalignment and such resonators have been utilised for their ruggedness in military applications. The key feature of these resonators are the complex field distributions which are experimentally observed and the output spatial modes of this laser are represented by Petal-like and Kaleidoscope modes[1,2]. Comprehensive models of these resonators exist where all aspects of the resonator are explored in generating such profiles, however very little work has gone into determining the composition of the electric field distributions and the physical properties of such beams.

Higher-order Laguerre-Gaussian modes and in particular Laguerre-Gaussian $TEM^{*}_{0,l}$ modes have been extensively studied for a variety of optical applications. These modes are generated by a superposition of two $TEM_{0,l}$ modes where one is rotated $\pi/2$ with respect to the other. They possess well defined orbital angular momentum along the optical axis for non zero values of l[3]. Laguerre-Gaussian $TEM_{0,l}$ modes have been reported to be linked with the formation of Petal-like transverse modes[4]. Chen[4] explores pumping a microchip laser with a hollow beam profile allowing for a single $TEM_{0,l}$ mode to oscillate and in the event of double pumping, for pump regions which are well separated, the characteristic modes will be superimposed to form a petal pattern output profile. These profiles have been reported to be experimentally generated by use of photorefractive oscillators[5], nonlinear interferometers[6], saturation of nonlinear media[7], pumping a microchip laser with a dark hollow beam[4,8] and suppressing low order transverse mode oscillation by defecting the rear mirror with a spot in a flat-flat cavity[9] . These techniques, and in particular[4,8,9] are extremely successful in petal pattern generation, however are limited in the sense that the fundamental propagation of the petal structures have not been investigated. We now further consider the possibility of a coherent superposition of Laguerre-Gaussian $TEM_{0,l}$ modes in the generation of Petal-like transverse modes similar to that observed in porro prism resonators.

Coherent superposition of laser beams has been comprehensively researched, where high brightness while maintaining good beam quality is the ultimate objective. Obtaining a successfully superimposed beam; one requires a minimum of two laser distributions to be efficiently phase locked so as to prevent excessive losses. Ideally, phase locking of several individual distributions should be self produced within a laser cavity and this has been shown to be possible by use of Michelson interferometers[10,11], Fourier Transform resonators[12,13], phase diffractive components[14], phase conjugation[15], intra-cavity interferometric beam combiners[16-19] and intra-cavity fiber couplers[20]. The above techniques are successful in obtaining efficient phase locking; however, most of these techniques consider phase locking of multiple Gaussian distributions but do not consider transverse modes due to the coherent superposition of higher-order modes.

In this paper we consider an alternative experimental approach to generate Petal-like transverse modes. We propose that these Petal-like profiles are acquired by coherently superimposing two Laguerre-Gaussian modes of zero radial order but opposite azimuthal order, $TEM_{0,\pm l}$. Experimental procedures are carried to verify that this hypothesis is correct. Visually based comparisons are drawn between the experimental intensity profiles and numerically simulated intensity profiles and a comparison of the beam quality factor and inner product interaction is carried out between experimental data and numerical data. The basis of the numerical research is presented in section (2) and the experimental procedures follow in section (3). An analysis and comparison of the Petal-like transverse modes with the numerical simulations are presented in section (4).

2. COHERENT SUPREPOSITION OF LAGUERRE-GAUSSIAN MODES

A coherent addition of higher-order modes is only applicable to beams which are mutually coherent, that is, that they oscillate with the same frequency which allows for the electric fields of the modes to be simply added together. We are particularly interested in the addition of two Laguerre-Gaussian $TEM_{p,l}$ modes, where p is the radial order and l is the azimuthal order for which the electric field, E_p^l, of the $TEM_{p,l}$ mode is given as[21]

$$E_p^l = \frac{E_0}{\sqrt{1+(z/z_0)^2}} \exp\left(\frac{-r^2}{w_0^2(z)} - \frac{ikr^2}{2R(z)}\right) \exp\left(-i(2p+l+1)\arctan\left(\frac{z}{z_0}\right)\right) \times \left(\frac{\sqrt{2}r}{w_0(z)}\right)^{|l|} L_p^l\left(\frac{2r^2}{w_0^2(z)}\right) \exp(il\phi) \tag{1}$$

where E_0 is the initial electric field, z is the propagation distance, z_0 is the Rayleigh range, $R(z)$ and $w_0(z)$ are the radius of curvature and beam width of a Gaussian beam respectively, r and ϕ are the radial and azimuthal coordinate respectively and L_p^l is the generalised Laguerre polynomial. In the case of the Petal-like transverse modes, $TEM_{0,\pm l}$, we consider the addition of two Laguerre-Gaussian modes both of zero radial order but having an opposite azimuthal order. The phase component of Eq. (1) is largely affected by the opposing l values in the addition of the two fields. Upon adding the electric fields of $TEM_{0,+l}$ and $TEM_{0,-l}$ modes the following superimposed field, $E_0^{\pm l}$, is obtained

$$E_0^{\pm l} = E_0^{+l} + E_0^{-l} = \frac{E_0}{\sqrt{1+(z/z_0)^2}} \exp\left(\frac{-r^2}{w_0^2(z)} - \frac{ikr^2}{2R(z)}\right)\left(\frac{\sqrt{2}r}{w_0(z)}\right)^{|l|} \times \left(\exp\left(-i\left(l\phi + (2p+l+1)\arctan\left(\frac{z}{z_0}\right)\right)\right) + \exp\left(i\left(l\phi - (2p+l+1)\arctan\left(\frac{z}{z_0}\right)\right)\right)\right) \tag{2}$$

The number of petals within the intensity profile is given as $2l$. The determination of the beam quality factor is a necessity as it provides fundamental information about the transverse mode and we perform this numerically. We firstly

determine the electric field of the Petal-like transverse modes at two positions in the far field by use of the Fresnel diffraction integral which reads as

$$E_2 = iN\exp(-ikL)\int_0^{2\pi}\int_0^1 \exp\left(-i\pi N\left(r_1^{*2} + r_2^{*2} - 2r_1^{*2}r_2^{*2}\cos(\phi_1 - \phi_1)\right)\right)\times E_1\left(r_1^*, \phi_1\right)r_1^* dr_1^* d\phi_1 \tag{3}$$

where N is the Fresnel number, L is the distance at which the field is considered, E_1 is the initial electric field, r_1^* and r_2^* are the normalised radial coordinates (normalised to the aperture radius) at the initial position and at position L respectively and ϕ_1 and ϕ_2 is the normalised azimuthal coordinates at initial position and at position L respectively . The expressions for the beam width, beam divergence and beam quality factor from second order intensity moments are given in Eqs. (4a) – (4c) respectively and read as follows[21]

$$\left\langle w_x^2 \right\rangle = \frac{4}{P_N}\int_{-\infty}^{\infty}\int_{-\infty}^{\infty} x^2 \left|E(x,y)\right|^2 dxdy \tag{4a}$$

$$\theta = \arctan\left(\frac{w_2 - w_1}{2D}\right) \tag{4b}$$

$$\left[\left\langle w_0^2 \right\rangle\left\langle \theta \right\rangle\right]_{general} = M^4\frac{\lambda^2}{\pi^2} \tag{4c}$$

where P_N is a normalisation factor, w_2 and w_1 are the calculated beam widths in the far field where w_2 is the larger of the two and D is the distance between the aforementioned beam widths. The beam waist, w_0 of the superimposed field may be calculated from Eq. (4a) where the electric field is the starting superimposed field.

3. EXPERIMENTAL SETUP

There are a variety of experimental approaches used to obtain Petal-like transverse modes as indicated in the section (1). Here we consider a plano-concave solid-state laser resonator which is end-pumped with a multi-mode fiber coupled diode. In order to successfully obtain $TEM_{0,\pm l}$ modes we are required to generate higher order Laguerre-Gaussian $TEM_{0,l}$ modes. This is achievable by inserting a thin opaque metal disk a very short distance away from the plane mirror of the cavity where the disk is large enough to completely obstruct Gaussian beam propagation and suppress lasing just above threshold in an open cavity. The insertion of the disk into the cavity allows for the selection of circular symmetric modes and at high input pump powers, higher-order Laguerre-Gaussian $TEM_{0,l}$ modes are able to oscillate. Mode competition within a multi-mode solid-state laser cavity results in the mode having the lowest loss allowed to propagate as the output. The modes which are superimposed to form the Petal-like transverse modes have identical losses and thus one is not able to differentiate between them within the laser cavity. To obtain an output for a stable cavity, these two modes are coherently added and propagate as Petal-like transverse modes. The phase locking required for coherent superposition is self produced within the cavity which is an ideal case as excessive losses are alleviated. The experimental setup is presented in Fig. 1.

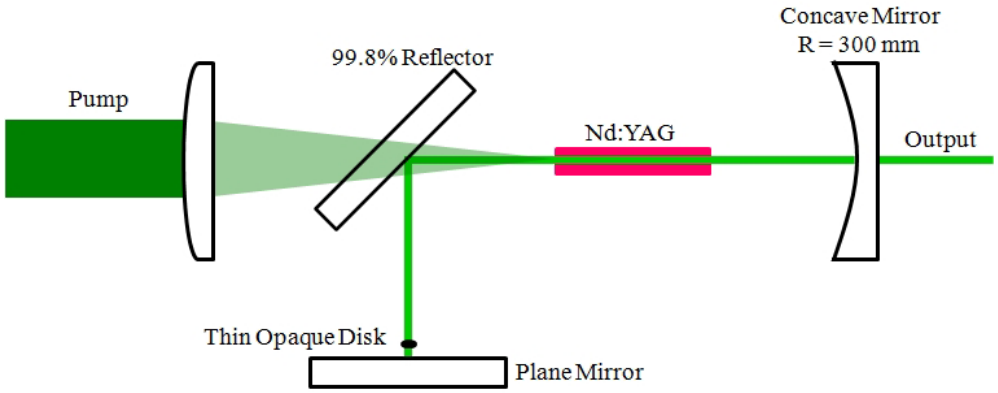

Figure 1: Experimental setup where an Nd:YAG solid-state medium is end pumped with a multi-mode fiber coupled diode and the output is viewed on a Spiricon CCD device.

The *g* parameter of the resonator was chosen to be 0.1 for a concave output coupler of 300 mm curvature. The gain medium, Nd:YAG (30mm x 4 mm rod), was end-pumped with a Jenoptik (JOLD-75-CPXF-2P W) 75 W multi-mode fiber-coupled diode and the beam profile was recorded on a CCD device (Spiricon LBA-USB L130). It is notably important to observe that the cavity is L-shaped in Fig. 1, as this allowed for the pump beam within the gain medium to remain bell shaped as there is no interference from the thin disk. The opaque disk is mounted on a plate of glass which has minimal round trip losses.

A standard beam profiling technique was used to determine the beam quality of the Petal-like modes. Upon focusing the beam through a lens, a CCD device was used to scan the beam profile along the propagation axis to determine the beam width. The obtained beam widths were then plotted against some distance away from a chosen reference position, namely the focusing lens. Upon fitting this curve with a second order polynomial, as in the example presented in Fig.2, the coefficients from the fit were used to determine the beam waist position, beam waist width and the beam quality factor. The global beam width obtained from the CCD device data is used as opposed to beam widths in the *x* and *y* planes due to the circular symmetric numerically generated profiles.

An inner product phase interaction experiment was performed where we considered the $TEM_{0,\pm l}$ modes interacting with a $TEM_{0,l}$ mode. A Spatial Light Modulator (SLM) was addressed with the phase array of a $TEM_{0,l}$ mode for a variety of l values and this allowed for an interaction with the incident Petal-like beam. The Fourier transform of this interaction was performed on the plane of the SLM (Holoeye HEO 1080P) by a thin lens. We propose that the Petal-like transverse modes are a linear combination of Laguerre-Gaussian $TEM_{0,l}$ modes.

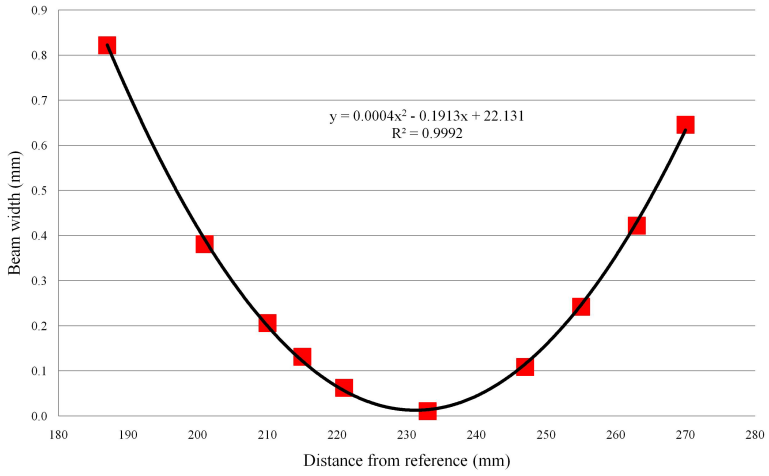

Figure 2: Polynomial fit of beam widths used to determine the beam quality factor of the petal like transverse mode.

4. RESULTS AND DISCUSSION

The Gaussian beam width on the plane mirror in an unperturbed cavity was calculated to be 174.6 μm and the opaque disk was chosen to be 200 μm in diameter. This ensured sufficient losses at lower input powers; such that at higher powers the gain was large enough to sustain lasing on specific modes. Figs. 3a – 3e illustrate the intensity profiles of the Petal-like output beams which were generated by use of the system in Fig. 1. The increase in the number of petals in the subsequent images are a direct result of an increase in the input pump power, hence an increase in gain. These images are compared to numerically simulated intensity profiles which are given in Figs. (3f) – (3j) which were generated by use of Eq. (2). These profiles look remarkably alike and we thus perform a comparison of visually based aspects.

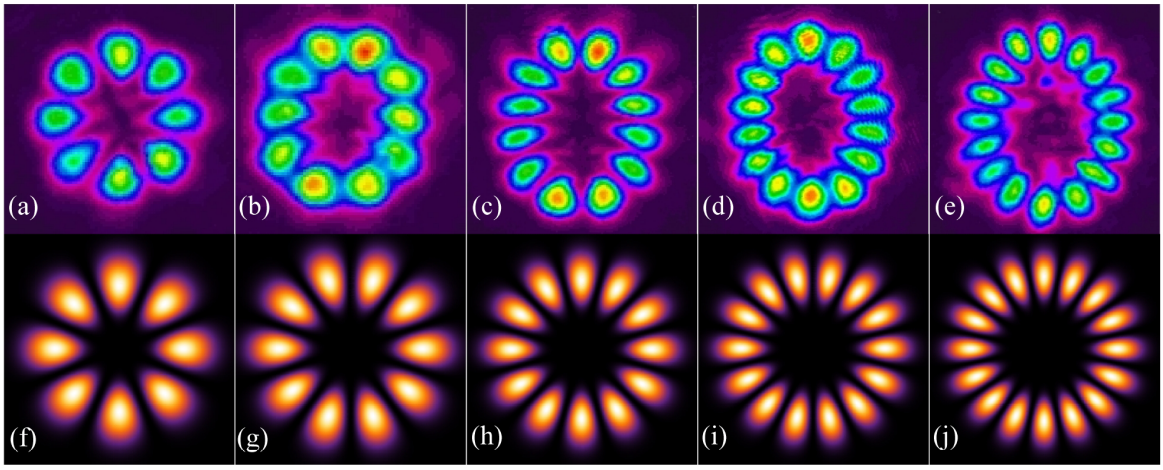

Figure 3: A comparison between experimentally generated Petal-like transverse modes, (a) – (e), and numerically simulated profiles (f) – (j) where the azimuthal order, *l*, in (a) is 4 and increases in unit value for the subsequent experimental images.

We generate numerical intensity profiles which have the same beam width as compared to their corresponding experimental images. There are three distinctive tests which may be performed; peak to peak petal diameter, angle between adjacent petals and peak to peak distance between adjacent petals. We have chosen the first two tests to perform as the angle between the adjacent petals incorporates the peak to peak distance between the petals and Fig. 4 illustrates what is considered in the two tests. An image tool (ImageJ) is used to perform the tests where an arbitrary value of intensity is assigned to each pixel corresponding to a specific colour. In the determination of the peak to peak petal diameter, a single line is drawn through the centre of the two petals of interest provided that the line passes through the midpoint of the image. We are able to retrieve, from an intensity plot generated from the drawn line, the distance between the two peaks as indicated in Fig. 4a. From the lines drawn in Fig. 4a we are then able to determine the angle between adjacent petals as shown in Fig. 4b. These comparisons are compared graphically in Fig. 5 and Fig. 6 for the peak to peak petal diameter and angle between adjacent petals respectively.

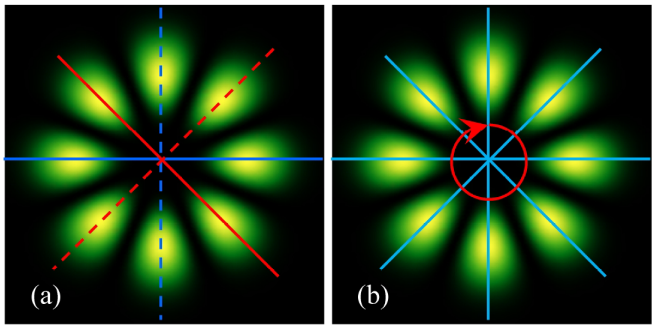

Figure 4: An illustration of the two visually based comparisons, (a) Peak to peak petal diameter and (b) Angle between adjacent petals, which are performed on numerically simulated intensity profiles and experimental data.

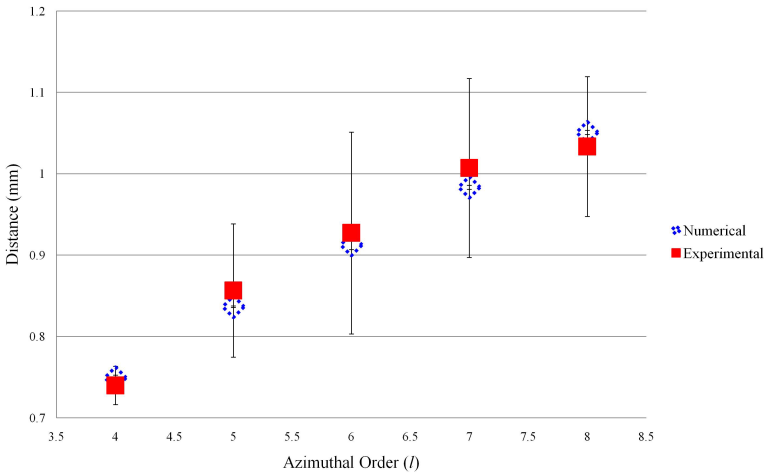

Figure 5: Comparison between numerical and experimental determination of the peak to peak petal diameter by use of an image tool.

There is a strong correlation between the numerical and experimental comparisons presented in Fig. 5 and Fig. 6 as the experimental data overlap extremely well with the numerical predictions particularly in the case of the determination of the angle between adjacent petals. These visual comparisons give a promising basis for the experimental determination of the beam quality factor of the Petal-like transverse modes. As indicated in section (2) and by the use of Eq. (3), the electric field of any given starting field may be determined at a specific position in the far field. This may be used in conjunction with Eqs. (4a) – (4c) to determine the beam width, beam divergence and beam quality factor respectively.

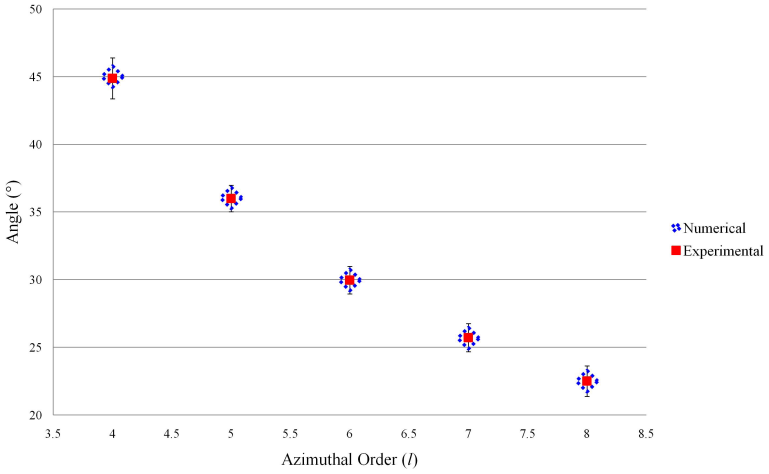

Figure 6: Comparison between numerical and experimental determination of the angle between adjacent petals by use of an image tool.

Numerically the beam quality factor is determined by obtaining the electric field at two positions, L_1 = 8 m and L_2 = 10 m in the far field by use of Eq. (3). We then plot these electric fields on independent graphs and fit them with a twentieth order polynomial. This polynomial is used with Eq. (4a) to determine the two beam widths respectively. Eq. (4b) and (4c) are then used to determine the numerical beam quality factor. To test that this numerical approach is viable in the determination of the beam quality factor for the $TEM_{0,\pm l}$ modes, we perform the simulation on Laguerre-Gaussian $TEM_{0,l}$ modes and compare this to the presently existing analytical expression of the beam quality factor for $TEM_{p,l}$ modes , $M^2 = 2p + l + 1$. This comparison is presented in Fig. 7 and shows an exceptional relationship between the simulation and the analytical result. We thus use this numerical method and compare the results to the experimental results which are shown in Fig. 8, where the experimental method used is provided in section (3).

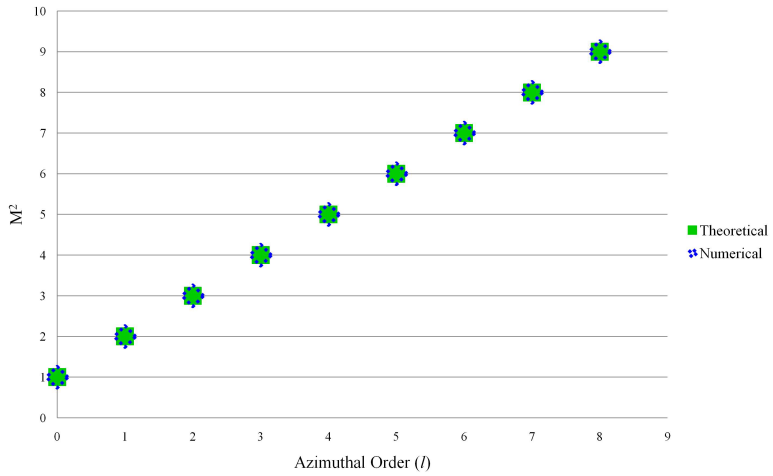

Figure 7: Determination of the beam quality factor by numerical simulation and by analytical expression for Laguerre-Gaussian $TEM_{0,l}$ modes.

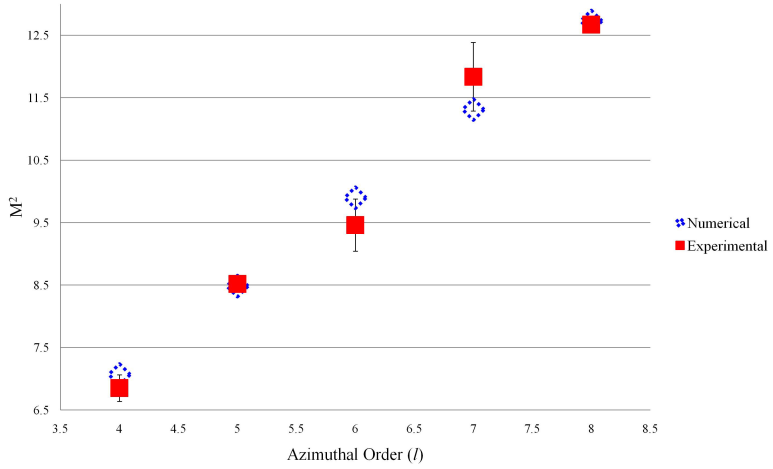

Figure 8: Numerical prediction of the beam quality factor as compared to an experimental approach for $TEM_{0,\pm l}$ modes.

The data presented in Fig. 8 compare exceedingly well and we are thus able to determine the propagation of such Petal-like transverse modes. A numerical determination of the intensity at the centre of the beam in the Fourier plane after the inner product phase interaction revealed a very interesting observation. By varying the azimuthal component, l, of the conjugate phase, $TEM_{0,l}$, from -10 to +10, we find that in the Fourier plane after the phase interaction, the intensity at the midpoint is null for values of l which do not correspond to the composition of the incident field, $TEM_{0,\pm l}$, and is non zero for all other values of l. This is carried out experimentally where the incident field is a $TEM_{0,\pm 6}$ mode and the phase interaction occurs with an SLM which has been addressed with a $TEM_{0,l}$ phase. The azimuthal order of the phase on the SLM is varied from -10 to +10 and at the Fourier plane of the SLM we anticipate a positive signal at the midpoint of the beam for l of -6 and +6 and null for every other value of l.

5. CONCLUSION

We have successfully demonstrated the generation of Petal-like transverse modes in an end pumped plano-concave solid-state resonator cavity by the introduction of a thin metal opaque disk. The disk suppresses lower order oscillation and induces the propagation of higher order circular symmetric modes. These modes which are observed in solid-state porro-prism laser resonators are now better understood in terms of propagation characteristics. Fundamental visually based

tests have been performed on these modes namely the determination of the peak to peak petal diameter and the angle between adjacent petals. The beam quality factor which is an essential propagation characteristic is numerically calculated and this compares exceptionally well to experimental data. We have effectively demonstrated a phase interaction between a Petal-like transverse mode and its conjugate which is unique to modes which are a linear combination of an orthogonal set. The excellent correlation between the numerical and experimental data implies that the Petal-like transverse modes are a result of a coherent superposition of two Laguerre-Gaussian $TEM_{0,l}$ modes.

ACKNOWLEDGEMENTS

We wish to thank Dr Stef Roux, Dr Igor Litvin and Mrs Liesl Burger for the invaluable discussions and useful advice.

REFERENCES

[1] Litvin I. A., Burger L. and Forbes A., "Petal-like modes in Porro prism resonators," Opt. Express **15**(21), 14065-14077 (2007).
[2] Burger L. and Forbes A., "Kaleidoscope modes in large aperture Porro prism resonators," Opt. Express **16**(17), 12707 – 12714 (2008).
[3] Allen L., Beijersbergen M. W., Spreeuw R. J. C. and Woerdman J. P., "Orbital angular momentum of light and the transformation of Laguerre-Gaussian laser modes," Phys. Rev. A **45**(11), 8185 – 8190 (1992).
[4] Chen Y. F. and Lan Y. P., "Laguerre-Gaussian modes in a double-end-pumped microchip laser: superposition and competition," J. Opt. B: Quantum Semiclass. Opt. **3**, 146 – 151 (2001).
[5] Arecchi F. T., "Optical morphogenesis: Pattern formation and competition in nonlinear optics," Physics D **86**, 297 – 322 (1995).
[6] Akhmanov S. A., Vorontsov M. A., Ivanov V. Yu., Larichev A. V. and Zheleznykh N. I., "Controlling transverse-wave interactions in nonlinear optics: generation and interaction of spatiotemporal structures," J. Opt. Soc. Am. B **9**(1), 78 – 90 (1992).
[7] Grynberg G., Maître A. and Petrossian A., "Flowerlike patterns generated by a laser beam transmitted through a Rubidium Cell with Single Feedback Mirror," Phys. Rev. Lett. **72**(15), 2379 – 2383 (1994).
[8] Chen Y. F. and Lan Y. P., "Dynamics of the Laguerre Gaussian $TEM^{*}_{0,l}$ mode in a solid-state laser," Phys. Rev. A **63**, 3807 (2001).
[9] Ito A., Kozawa Y. and Sato S., "Generation of hollow scalar and vector beams using a spot-defect mirror," J. Opt. Soc. Am. A **27**(9), 2072 – 2077 (2010).
[10] DiDomenico M., "A single-frequency TEM_{00}-mode gas laser with high output power," Appl. Phys. Lett. **8**(1), 20 – 22 (1966).
[11] Sabourdy D., Kermène V., Desfarges-Berthelemot A., Vampouille M. and Barthélémy A., "Coherent combining of two Nd:YAG lasers in a Vernier-Michelson-type cavity," Appl. Phys. B **75**, 503 – 507 (2002).
[12] Philipp-Rutz E. M., "Spatially coherent radiation from an array of GaAs lasers," Appl. Phys. Lett. **26**(8), 475 – 477 (1975).
[13] Menard S., Vampouille M., Desfarges-Berthelemont A., Kermene V., Colombeau B. and Froehly C., "Highly efficient phase locking of four diode pumped Nd:YAG beams," Opt. Comm. **160**, 344 – 353 (1999).
[14] Leger J. R., Swanson G. J. and Veldkamp W. B., "Coherent laser addition using binary phase gratings," Appl. Opt. **26**(20), 4391 – 4399 (1987).
[15] Desfarges A., Kermene V., Colombeau B., Froehly C. and Vampouille M., "Multiple-beam, spatially mode-locked photoreflective oscillator," Opt. Comm. **127**, 372 – 380 (1996).
[16] Ishaaya A. A., Shimshi L., Davidson N. and Friesen A. A., "Coherent addition of spatially incoherent light beams," Opt. Express. **12**(20), 4929 – 4934 (2004).
[17] Ishaaya A. A., Davidson N., Shimshi L. and Friesen A. A., "Intracavity coherent addition of Gaussian beam distributions using a planar interferometric coupler," Appl. Phys. Lett. **85**(12), 2187 – 2189 (2004).
[18] Ishaaya A. A., Eckhouse V., Shimshi L., Davidson N. and Friesen A. A., "Intracavity coherent addition of single high-order modes," Opt. Lett. **30**(14), 1770 – 1772 (2005).
[19] Eckhouse V., Ishaaya A. A., Shimshi L., Davidson N. and Friesen A. A., "Intracavity coherent addition of 16 laser distributions," Opt. Lett. **31**(3), 350 – 352 (2006).

[20] Shirakawa A., Saitou T., Sekiguchi T. and Ueda K., "Coherent addition of fiber lasers by use of a fiber coupler," Opt. Express **10**(21), 1167 – 1172 (2002).
[21] Hodgson N. and Weber H., [Laser Resonators and Beam Propagation], Springer, New York, Chap. 2 and 5 (2005).